A TWO-DIMENSIONAL PARABOLIC MODEL FOR VERTICAL ANNULAR TWO-PHASE FLOW

F. M. Fernández, fernandez.lubnicki@gmail.com
A. Alvarez Toledo, alvareztoledoa@yahoo.com
E. E. Paladino, emilio@ct.ufrn.br

Graduate Program in Mechanical Engineering, Universidade Federal de Rio Grande do Norte, Natal, RN 59072-970, Brazil

Abstract. *This work presents a solution algorithm for predicting hydrodynamic parameters for developing and equilibrium, adiabatic, annular, vertical two-phase flow. It solves mass and momentum transport differential equations for both the core and the liquid film across their entire domains. Thus, the velocity and shear stress distributions from the tube center to the wall are obtained, together with the average film thickness and the pressure gradient, making no use of empirical closure relations nor assuming any known velocity profile to solve the triangular relationship in the liquid film. The model was developed using the Finite Volume Method and an iterative procedure is proposed to solve all flow variables for given phase superficial velocities. The procedure is validated against the analytical solution for laminar flow and experimental data for gas-liquid turbulent flow with entrainment. For the last case, an algebraic turbulence model is used for turbulent viscosity calculation for both, liquid film and gas core.*

Keywords: *Gas-liquid flow, Annular flow, Finite Volume Method, Parabolic flow*

1. INTRODUCTION

Two-phase gas-liquid annular flow is one of the most common patterns encountered in internal flows in the process, nuclear and oil industries. This pattern occurs at moderate to high gas superficial velocities and it is characterized by the existence of a liquid film adjacent to the wall and a gas core flowing in the center of the duct. A wavy interface exists between both phases and its morphology depends on the gas and liquid mass flow rates. Two types of waves are present at the interface, briefly described as low amplitude or ripple waves and large amplitude or disturbance waves. It has been shown (see for example, Azzopardi (1997), Hewitt & Whalley (1989)) that the latter are responsible for the entrainment phenomenon; liquid droplets are ejected into the gas core when the crests of the disturbance waves are sheared-off by the gas. Also, droplets can be re-deposited into the liquid film. For large duct lengths the mass transfer between the gas core and liquid film will eventually reach equilibrium where entrainment and deposition rates become equal and there are no further bulk variations of flow parameters in the axial direction. Still, an entrained fraction will always be present.

As pointed out by Hewitt & Whalley (1989), given the independent variables (fluid properties, channel geometry and total liquid and gas flow rates), annular flow modeling consists in the calculation of three dependent variables, namely liquid film flow rate, mean film thickness, and pressure gradient. After a review of the existing literature, there were found different ways to model the flow of both phases and their interaction.

One of the most common approaches assumes that the velocity profile within the liquid film is obtained from logarithmic wall law relations, similar to those for single phase turbulent flow (Moeck & Stachiewicz (1972); Dobran (1983); Adechy & Issa (2004); Kishore & Jayanti (2004)). Others use empirical closure relations for the interfacial shear stress or interfacial friction factor (Whalley & Hewitt (1978); Fu & Klausner (1997) ; Okawa & Kataoka (2005); Fan et al. (2006); Peng (2008)). Some researchers (Moeck & Stachiewicz (1972); Dobran (1983)) presented more sophisticated models considering the liquid film as to be divided into two sub-layers: a continuous liquid layer next to the wall which responds to the law-of-wall, and a wavy one next to the liquid-gas interface which makes use of a correlation for friction factor in rough tubes to obtain the interfacial shear stress.

Concerning the gas core modeling, it is usually treated as an homogeneous mixture of gas and entrained liquid droplets, not considering slip between both phases (Dobran (1983); Kishore & Jayanti (2004)). Empirical correlations are used to predict the fraction of liquid entrained which is needed to compute the droplet-laden gas core density, viscosity and void fraction, based on homogeneity hypothesis. More complex models (Moeck & Stachiewicz (1972); Antal *et al.* (1998); Adechy & Issa (2004)) consider slip between liquid droplets and gas phase. The interaction of gas core with liquid film is usually modeled considering the interface as a rough surface and its effects are introduced through a friction factor correlation for rough walls or modifying the wall function, used to impose the boundary condition in turbulence models, to take the effect of roughness into account. This approach works better for gas-liquid flow with high superficial velocities, where films are very thin and film/core viscosity ratio is high.

Additionally, a number of one-dimensional approaches have been also presented in literature. Most successful ones are based on multi-fluid modeling of annular-dispersed flow (Fossa (1995); Alipchenkov *et al.* (2004)), treating each field (liquid film, droplets and gas core) as individual fluids and using empirical correlations to account for interfacial mass, momentum and energy transfer among them.

This work presents a new solution algorithm which, unlike mentioned approaches, makes no use of empirical closure correlations to relate shear stresses, pressure gradient and film thickness nor assumes any velocity profile for the liquid film. Instead, the effect of the dispersed droplets in the core and the wavy interface are taken into account in the turbulence model. It has been shown these increase turbulence intensity and, hence, pressure gradient. The model provides an accurate, simple and complete numerical computation of all the hydrodynamic parameters requiring just gas and liquid mass flow rates as input data to solve mass and momentum conservation equations. As the model is based on the solution of conservation equations with its boundary conditions and interfacial constraints, its application is broad, allowing for instance, the solution of developing annular flow for non-equilibrium case. Its extension for heat transfer computations is also straightforward. The success of the algorithm relies on two main features. First, the coupled solution of the liquid film and gas core velocity fields, which inherently satisfies the continuity of the velocity and shear stress fields at the interface, and, second, the pressure gradient calculation through an iterative procedure based on the fulfillment of the global mass conservation of the gas core. Then, no use is made of the global force balance that relates pressure gradient and wall shear stress and the mass conservation in liquid film is used to calculate the film thickness.

The model is validated for laminar flow against the analytical solution for core-annular flow of two immiscible fluids in a circular pipe and for turbulent flow with the experimental results of Wolf *et al.* (2001). Their measured data for pressure gradient, film thickness and wall shear stress is compared with those predicted by the model for fully-developed conditions and for developing annular flow. In these cases, the algebraic turbulence model presented by Cioncolini *et al.* (2009) was used for eddy viscosity calculation in liquid film and gas core.

2. MODEL DESCRIPTION

The proposed model divides the flow domain in two distinct regions shown in Figure 1, the liquid film (lf) and the gas core (gc); the former is treated as a continuous, fully turbulent layer having no entrained bubbles, with a mean film thickness δ. The wavy nature of the interface and its effects on the interfacial shear stress is taken into account through the turbulence model as will be described later. The gas core is considered to have liquid droplets entrained.
Modeling is carried out under the following assumptions:

1. Steady-state, co-current, vertical, annular flow.
2. Flow is assumed to be axis-symmetric. Then, film thickness is assumed to be constant in angular coordinate.
3. Entrainment and deposition processes have not reached equilibrium conditions, meaning that there is mass and momentum transfer between liquid film and gas core.
4. There is no slip between the gas and the entrained liquid droplets.
5. The properties of the core mixture are assumed to change along the axial coordinate due to entrainment and deposition, but the radial distribution of droplets is homogeneous
6. The gas phase is considered incompressible, but due to entrainment and deposition the gas core density is variable along the axial coordinate.

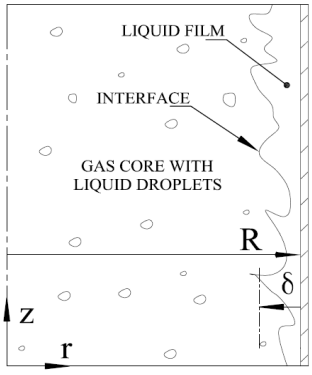

Figure 1: Model description

2.1 Governing Equations

Considering the parabolic hypothesis, i.e., the diffusive momentum fluxes in the axial direction are much smaller than the radial ones, the time-averaged linear momentum equations for the gas core and the liquid film are given by,

$$\frac{\partial}{\partial z}\left(\rho_{gc}u_{gc}u_{gc}\right)+\frac{\partial}{\partial r}\left(\rho_{gc}v_{gc}u_{gc}\right)=-\frac{\partial p}{\partial z}+\frac{1}{r}\frac{\partial}{\partial r}\left(\mu_{eff,gc}\,r\,\frac{\partial u_{gc}}{\partial r}\right) \qquad 0<r<R-\delta \tag{1}$$

$$\frac{\partial}{\partial z}\left(\rho_{lf}u_{lf}u_{lf}\right)+\frac{\partial}{\partial r}\left(\rho_{lf}v_{lf}u_{lf}\right)=-\frac{\partial p}{\partial z}+\frac{1}{r}\frac{\partial}{\partial r}\left(\mu_{eff,lf}\,r\,\frac{\partial u_{lf}}{\partial r}\right)\qquad R-\delta<r<R \tag{2}$$

In developing annular flow, when the gas density is constant, three mechanisms will affect the momentum balance in the gas core:

1. The local acceleration which will affect the profile shape
2. The global acceleration due to the variation of the film thickness
3. The variation of the core density, which is function of entrained liquid

Kishore & Jayanti (2004) showed that for the experimental conditions covered within data of Wolf et al. (2001) the velocity profiles scarcely change in the length range where data were taken. This means that the acceleration due to changes in velocity profiles is negligible. Actually, the effects of the so called "entrance region" in the context of single phase flows would be very difficult to measure in the case of multiphase flows, as flat profiles condition would be very difficult to generate for a specific flow pattern. For instance, the annular pattern in Wolf et al. (2001) experiments is generated by injecting liquid through porous walls at about ten duct diameters after the air inlet, so some developing (if not "full") happens in the air velocity profiles previous to the onset of the annular flow. Therefore, the momentum variations due to the changes on velocity profile are neglected, and so is the radial component of the velocity vector. The acceleration due to the variation of transversal area of gas core flow is proportional to the variation of the film thickness along the axis which is usually of order of a fraction of a millimeter per meter and can also be neglected. Nevertheless entrainment and deposition rates which are not at the equilibrium condition, modify the density of the gas core. Consequently, the momentum balance is affected by the mass exchange between liquid film and gas core. This phenomenon can also be viewed as the momentum transfer from liquid film to the gas core (or vice versa) due to entrainment (or deposition) of droplets, which are initially moving at a speed equal to that of the interfacial disturbance waves, and are accelerated to the core velocity (before eventual re-deposition). When droplets are sheared-off from the film these are gradually accelerated to the local gas velocity. Nevertheless, due to homogeneity hypothesis for the gas core, the droplet entrained assumes instantaneously the gas velocity. The effect of entrainment on momentum balance of the gas core is computed in a global way using the entrainment correlation of Kataoka *et al.*(2000) to obtain the entrained liquid fraction along the tube axis. It represents the integral effects of entrainment and deposition rates, then, the gas core density is calculated in every slice of the tube, under the homogeneous hypothesis, as shown in section 2.4 below. The momentum variation of the film is considered to be negligible.

The pressure gradient is shared by both phases and is assumed to change only in axial direction (constant in radial coordinate). Body forces are excluded from the linear momentum equation, assuming that their contribution is negligible as confirmed by Wolf *et al.* (2001).

The boundary conditions for equations (1) and (2) are given by:

$$\frac{du}{dr}=0\qquad r=0 \tag{3}$$

$$u=0\qquad r=R \tag{4}$$

The continuity of velocities and shear stresses at interface is respectively given by Eqs. (5) and (6).

$$u_{gc}(R-\delta)=u_{lf}(R-\delta)=u_I \tag{5}$$

$$\tau_{gc}\big|_{R-\delta}=\tau_{lf}\big|_{R-\delta}=\tau_I \tag{6}$$

The mass flows of gas core and liquid film are calculated by the integration of the velocity profiles as,

$$\dot{m}_{gc}=2\pi\rho_{gc}\int_0^{R-\delta}u(r)\cdot r\,dr \tag{7}$$

$$\dot{m}_{lf}=2\pi\rho_{lf}\int_{R-\delta}^{R}u(r)\cdot r\,dr \tag{8}$$

These relations represent the global mass conservation for the gas core and liquid film and are used, together with momentum conservation, in the solution algorithm for pressure gradient and film thickness calculation.

2.2 Finite Volume Integration

The momentum equation for each region is integrated in its corresponding domain using the Finite Volume technique. An independent mesh with a fixed number of volumes for each region allows refinement within the liquid film. The gas-liquid interface is positioned between the last gas-core volume (Ng) and the first liquid film volume

(Ng+1), as shown in Figure 2. Along the iterative procedure, the film thickness varies each time it is corrected, so *Δrl* and *Δrg* are adjusted since the number of volumes within liquid film and gas core is constant.

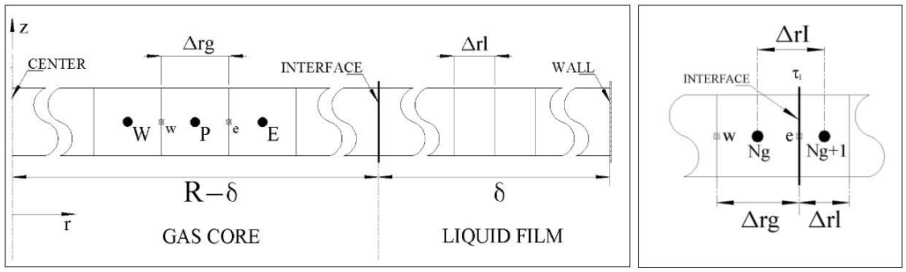

Figure 2: (a) Grids for gas core and liquid film domains – (b) Finite volumes contiguous to the interface

Integration of Eq. (1) in volume P (Figure 2) gives,

$$\underbrace{r_e\,\mu_{eff,gc}\left.\frac{du_{gc}}{dr}\right|_e}_{\tau_e} - \underbrace{r_w\,\mu_{eff,gc}\left.\frac{du_{gc}}{dr}\right|_w}_{\tau_W} = \frac{dp}{dz}(r_e^2 - r_w^2) + \left(u_{lf}u_{lf}\right)\frac{d\rho_{gc}}{dz}(r_e^2 - r_w^2) \qquad 0 < r < R-\delta \tag{9}$$

The second term of the r.h.s represents the momentum variation of the gas core due to entrainment. The use of central differencing scheme (CDS) for interpolation of the velocity gradients results in the following algebraic equation for the discrete momentum conservation within volume P,

$$A_p U_P + A_e U_E + A_w U_W = \quad B \tag{10}$$

To integrate Eqs. (1) and (2) within volumes contiguous to the interface, *Ng* and *Ng+1* in Figure 2-b, the continuity of interfacial stresses has to be ensured by finding a single expression to evaluate the interfacial shear stress in both volumes, as Eq. (11) illustrates.

$$\underbrace{\mu_{eff,gc}\left.\frac{du_{gc}}{dr}\right|_{R-\delta}}_{\tau e(Ng)} = \underbrace{\mu_{eff,lf}\left.\frac{du_{lf}}{dr}\right|_{R-\delta}}_{\tau w(Ng+1)} = \tau_I \tag{11}$$

To accomplish this, a procedure described in Patankar (1980) for media with non-uniform diffusion coefficient (say viscosity or conductivity) is used. An expression for an equivalent interfacial viscosity is derived out of the continuity of shear stress resulting in,

$$\mu_I = \left(\frac{1-f_I}{\mu_{eff,gc}} + \frac{f_I}{\mu_{eff,lf}}\right) \quad ; \quad f_I = \frac{\Delta rl}{\Delta rl + \Delta rg} \tag{12}$$

Then, the shear stress is obtained as,

$$\tau_I = \mu_I \left.\frac{du}{dr}\right|_I = \mu_I \frac{u_{Ng+1} - u_{Ng}}{\Delta r_I} \tag{13}$$

where

$$\Delta r_I = \frac{1}{2}\left(\Delta rg + \Delta rl\right) \tag{14}$$

The interpolation of the derivative at the interface is done by CDS using the velocities of interfacial volumes, Ng and Ng+1, as shown by Eq. (13).

The effective viscosity, which is a function of the radial position, is stored at the volume faces in a staggered grid. This simplifies discretization since the viscosities are required at the volume interfaces to calculate momentum fluxes. So, the dynamic viscosities can be written as:

$$\mu_{eff} = \begin{cases} \mu_{eff,gc} & 0 < r < R - \delta \\ \mu_{eff,lf} & R - \delta < r < R \\ \\ \dfrac{1 - f_1}{\mu_{eff,gc}} + \dfrac{f_1}{\mu_{eff,lf}} & R = \delta \end{cases} \tag{15}$$

where $\mu_{eff,gc}$ and $\mu_{eff,lf}$ are the effective viscosities that can be obtained by any turbulence model that is adequate for annular flow. For the case of laminar flow without entrainment the viscosities will simply be the ones of the liquid and gas (or "liquid core", in the case of liquid-liquid flows).

Velocity fields for liquid film and gas core are solved in a single matrix equation simultaneously, as schematically shown below, satisfying the momentum equations and boundary conditions together with velocity and shear stress continuity at the interface, for given pressure gradient and film thickness. The resulting matrix has three non zero diagonals and can be easily solved by the TDMA algorithm.

$$\begin{bmatrix} \mathbf{A}_{gc} & \ddots \\ \ddots & \mathbf{A}_{lf} \end{bmatrix} \begin{bmatrix} \mathbf{U}_{gc} \\ \mathbf{U}_{lf} \end{bmatrix} = \begin{bmatrix} \mathbf{B}_{gc} \\ \mathbf{B}_{lf} \end{bmatrix} \tag{16}$$

2.3 Turbulence Model

In order to make the model applicable to turbulent gas-liquid annular flows and validate the solution algorithm against available experimental data, the algebraic turbulence model proposed by Cioncolini *et al.* (2009) was selected to calculate eddy viscosities. This model treats the liquid film in an average way and the wavy nature of the interface is taken into account in the correlations proposed for turbulent viscosities, which were developed by the authors from a large experimental database. For the liquid film, the effective viscosity only depends on its thickness δ, and is calculated as,

$$\mu_{lf}^{eff} = \mu_l \sqrt{1 + 0.9 \times 10^{-3} \cdot (\delta^*)^2} \qquad \delta^* = \frac{\delta \cdot \rho_l \cdot \sqrt{\tau_w / \rho_l}}{\mu_l}$$

Regarding the gas core effective viscosity, it varies linearly with wall distance and inversely proportional to a constant ***a***.

$$\mu_{gc}^{eff} = \mu_{gc} \cdot \frac{y^*}{a} \qquad y^* = \frac{y \cdot \rho_{gc} \cdot \sqrt{\tau_w / \rho_{gc}}}{\mu_{gc}}$$

For the computation of the constant ***a***, the authors propose an average value of 4.2 ± 1.0 with an approximate standard deviation of 24%. In the present study, its value is set to 4.3.

The parameters needed to solve this model are the liquid and gas core fluid properties (ρ_l, ρ_{gc}, μ_l and μ_{gc}), and the wall shear stress. The last one is obtained by deriving the velocity profile and the gas core properties are calculated as explained in the next section.

Other turbulence models based on (time-averaged) Reynolds equations can be used, as long as they are based on turbulent viscosity and, of course, include the effects of the interface waves in an average way into the turbulent viscosity model.

2.4 Liquid entrainment and gas core properties

As this model solves developing and equilibrium annular flow, the entrainment correlation of Kataoka *et al.*(2000) was used for predicting the entrained liquid fraction *e*; it is valid for entrance region and under hydrodynamic equilibrium conditions, given by:

$$e = \left(1 - \exp\left(-1.87 \cdot 10^{-5} \zeta^2\right)\right) e_\infty \tag{17}$$

where ζ and e_∞ are the dimensional distance and the equilibrium entrained fraction, respectively, given by:

$$\zeta = \frac{(z/d)\,\mathrm{Re}_l^{0.5}}{We^{0.25}} \qquad e_\infty = \tanh\left(7.25 \cdot 10^{-7}\, We^{1.25}\, \mathrm{Re}_l^{0.25}\right) \tag{18}$$

where

$$We = \frac{\rho_g J_g^2 d}{\sigma}\left(\frac{\rho_l - \rho_g}{\rho_g}\right)^{0.33} \qquad \text{and} \qquad \mathrm{Re}_l = \frac{\rho_l J_l d}{\mu_l}$$

Out of the total gas and liquid mass flow rates $\dot{m}_g$ and $\dot{m}_l$, which are input data, and the fraction of liquid entrained calculated through Eq. (23), liquid entrained ($\dot{m}_{le}$), liquid film ($\dot{m}_{lf}$) and gas core ($\dot{m}_{gc}$) mass flow rates can be obtained as,

$$\begin{aligned} \dot{m}_{le} &= \dot{m}_l \cdot e \\ \dot{m}_{lf} &= \dot{m}_l - \dot{m}_{le} \\ \dot{m}_{gc} &= \dot{m}_g + \dot{m}_{le} \end{aligned} \tag{19}$$

Finally, the gas core fluid properties ρ_{gc} and μ_{gc} are calculated according to the homogeneous model as,

$$\begin{aligned} \rho_{gc} &= (1-\alpha)\rho_g + \alpha\rho_l \\ \mu_{gc} &= (1-\alpha)\cdot\mu_g + \alpha\cdot\mu_l \end{aligned} \tag{20}$$

where α is the droplet volume fraction:

$$\alpha = \frac{e\dot{m}_l/\rho_l}{e\dot{m}_l/\rho_l + \dot{m}_g/\rho_g} \tag{21}$$

The gas core density derivative appearing in the advective term of the momentum equation can be explicitly obtained deriving the expressions above, as:

$$\frac{\partial \rho_{gc}}{\partial z} = (\rho_l - \rho_{gc})\frac{\partial \alpha}{\partial z}$$

and

$$\frac{\partial \alpha}{\partial z} = \frac{\partial \alpha}{\partial e}\frac{\partial e}{\partial z}$$

The change in gas density due to decreasing pressure along flow development is neglected. Then,

$$\frac{\partial \rho_{gc}}{\partial z} = (\rho_l - \rho_{gc})\frac{\partial e}{\partial z}\frac{\alpha}{e}(1-\alpha) \tag{22}$$

3. SOLUTION ALGORITHM

The flow chart shown in Figure 4 summarizes the scheme of solution. The input data consists in mass flow rates of each phase, fluid properties, tube dimensions, initial conditions and numerical parameters such as convergence tolerance and mesh size. Initial values of pressure gradient and film thickness need to be guessed. These are corrected through an iterative procedure until the converged values are obtained.

For a given film thickness, the external loop starts calculating the position of the volume centers and faces for the whole domain, gas core and liquid film. Then, the fraction of liquid entrained is obtained from Eq. (18) and liquid film and gas core mass flow rates form Eqs. (19). The fluid properties of the gas core are calculated through Eqs. (20). For a given pressure gradient, the internal loop first calculates the effective viscosity, in this case using the turbulence model described in section 2.3. Then, system (16) is solved to obtain the velocity profiles of liquid film and gas core. With the last one , the gas core mass flow rate is obtained using Eq. (7) and the pressure gradient is adjusted to satisfy the known gas core flow rate through a procedure similar to the one proposed by Patankar & Spalding (1972). This algorithm uses the error between the flow rate calculated from the velocities obtained from momentum equations and the given value to correct the pressure gradient. This corrected value is inserted into the momentum equation and new velocities are obtained. This process is repeated until the total mass flow rate is satisfied. The wall shear stress required for effective viscosity computation, is updated within each pressure gradient correction iteration, since the velocity field changes. After convergence of the internal loop, the velocity fields and pressure gradient satisfy momentum equation for a given film thickness. Next, the liquid film thickness is corrected to satisfy the mass flow rate of the liquid film using Eq. (8). As the number of volumes in each domain is constant, values of Δrg and Δrl change, as well as the positions of volume

centers and faces. As the correction of δ affects the velocity field of both, gas core and liquid film, the algorithm re-enters the internal loop, to find the pressure gradient that satisfies momentum equation for the new film thickness. This process is repeated until convergence of the whole system, obtaining velocity fields, film thickness and pressure gradient that satisfy momentum and mass conservation equations (Eqs. (7) and (8)).

It is important to highlight that the coupled solution of liquid film and gas core velocity fields (Eq. (16)) satisfies the continuity of shear stress at the interface and provides a pressure gradient dependent upon the gas core mass flow rate. In turn, the pressure gradient is responsible for the liquid velocity field, which determines the wall shear stress. In this way, the intimate relationship between the wall shear stress and pressure gradient is fulfilled without explicitly making use of any equation to relate them within the solution process. This is one of the key points of the algorithm because the triangular relationship between the liquid film mass flow rate, the wall shear stress, and the film thickness is successfully solved making no use of empirical relations for wall or interfacial friction factor nor assuming any liquid film velocity profile.

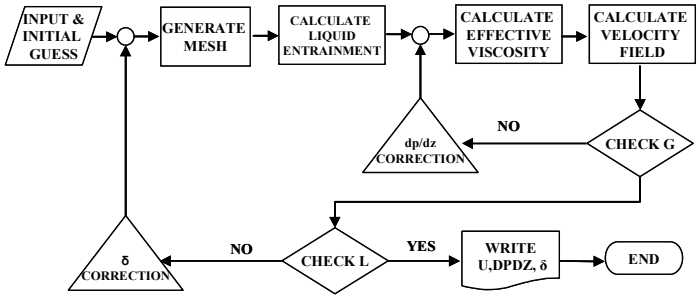

Figure 3: Numerical scheme flowchart

4. VALIDATION AND RESULTS

In order to validate the solution algorithm two comparisons are carried out. First, the solution for laminar flow is compared against the analytical solution which has as input the pressure gradient and film thickness. Then, the model is used to compute the film thickness and pressure gradient for fully-developed and for developing turbulent flow for given gas and liquid flow rates and compared with experimental data from Wolf *et al.* (2001)

4.1 Laminar, fully developed flow

Velocity profiles obtained from the implemented algorithm using laminar viscosities are compared with the analytical solution for fully developed laminar annular flow for known pressure gradient and film thickness. This comparison aims the verification of the algorithm for simpler cases where no empirical correlations for modeling complex phenomena, such as entrainment or turbulence, are necessary. The predicted pressure gradient and film thickness were substituted into Eqs. (23) and (24) to compare analytical profiles with the predicted ones

$$u_{gc}(r) = \frac{-dP/dz}{4\mu_{gc}}\left[(R-\delta)^2 - r^2\right] + \frac{-dP/dz}{4\mu_l}\left[R^2 - (R-\delta)^2\right] \tag{23}$$

$$u_{lf}(r) = \frac{-dP/dz}{4\mu_l}\left[R^2 - r^2\right] \tag{24}$$

Figure 4 shows the velocity profiles for two viscosity relations and different superficial velocity relations, comparing the results obtained with the presented algorithm and the analytical solution (Eqs. (23) and (24)). It can be observed that in all cases, the predicted profiles laid over the exact ones.

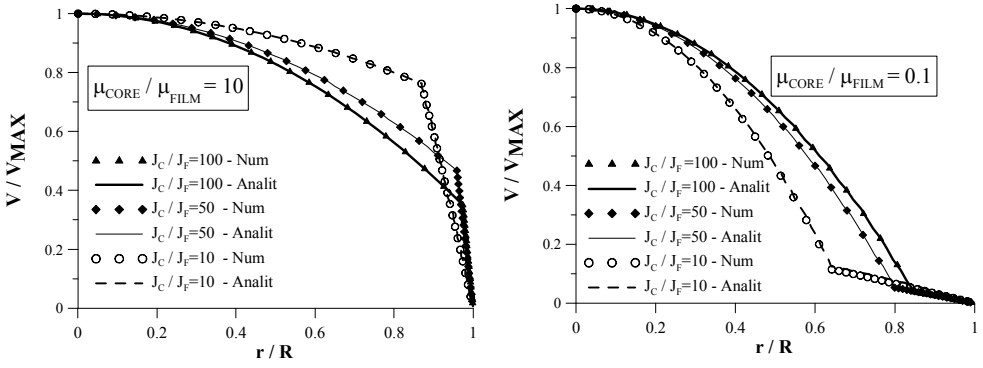

Figure 4 - Comparison of numerical and analytical results for different viscosity and superficial velocity relations

4.2 Fully developed turbulent flow

The model was used to obtain hydrodynamic parameters for air-water, fully-developed annular flow, for gas mass flow in the range of 71-154 kg/m^{2}s and liquid mass fluxes of 10-120 kg/m^{2}s, corresponding to the experimental data presented by Wolf *et al.*, 2001. Comparisons with experimental results are presented in Figure 5 for pressure gradient and film thickness.

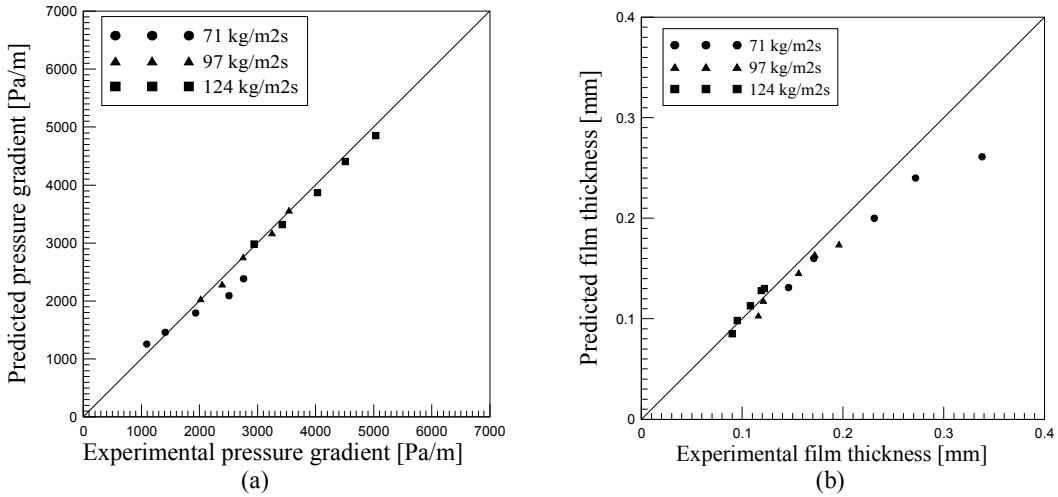

Figure 5- a) Predicted pressure gradient vs. experimental data of Wolf *et al.* (2001). b) Predicted film thickness vs. experimental data of Wolf *et al.* (2001).

Figure shows the variation of pressure gradient and mean film thickness with liquid mass flow rate for different gas flow rates, compared with experimental values from Wolf *et al.* (2001) . In general, results show good agreement with experimental data and deviations can be attributed to turbulence modeling or the entrainment correlation used for predicting the entrained liquid fraction. It is emphasized that it is not the objective of this work to produce or validate new physical models but to present a solution algorithm for mass and momentum conservation equations for annular flow in ducts, general enough to be capable of dealing with various physical models such as other turbulence models, entrainment correlations, state equations for variable fluid properties, etc., that can be added to enhance its prediction capacity.

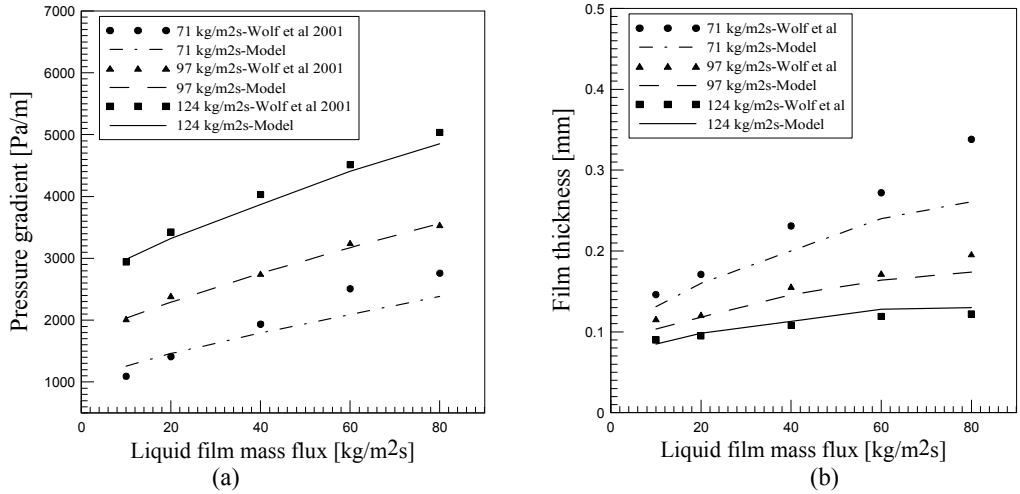

Figure 6- a) Pressure gradient vs. liquid mass flux, b) Film thickness vs. liquid mass flux , predicted and experimental Wolf *et al.* (2001).

4.3 Developing turbulent flow

The model was used to predict the flow parameters for developing annular flow, for flow conditions and mass rates as those of the experimental data presented by Wolf *et al.* (2001). Initial local pressure and mass fluxes are given. Even though the algebraic turbulence models used herein were developed for fully-developed flow, they were used for developing flow calculations, since no other suitable model was available by the time. Results are acceptable since some of the hypotheses assumed are still valid in quasi-equilibrium flow. Figure 7 shows the variation of liquid film mass flux, film thickness, pressure gradient and wall shear stress with axial distance for gas mass flux of 97 kg/m^{2}s and water mass flux of 40 kg/m^{2}s. All curves show quite good representation of the variables variations, with the exception of the wall shear stress. Even though the absolute error does not exceed 15%, the measured data show a steeper gradient towards the inlet region. As regards pressure gradient, the predicted values are within an error of 10% .Yet there is a slope change in the predicted curve which is unexpected according to experimental data.

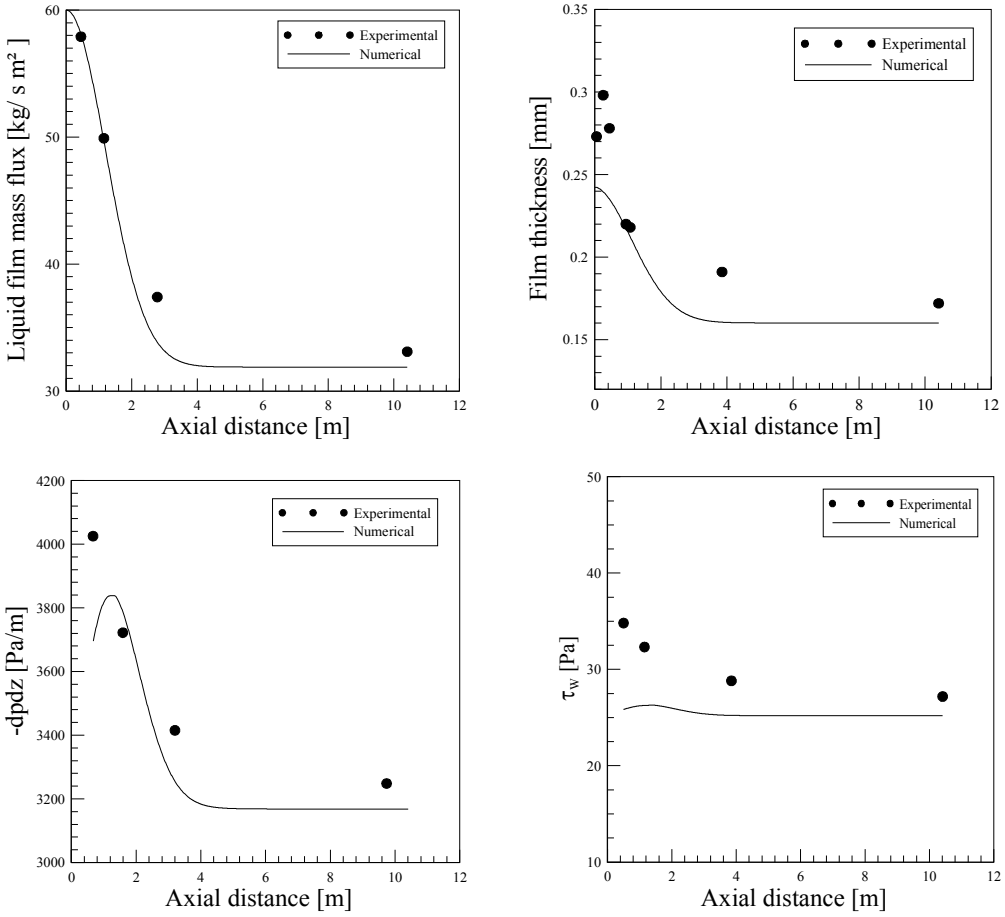

Figure 7- Liquid mass flux, film thickness, pressure gradient, and wall shear stress for developing annular flow. Predicted. vs. experimental data of Wolf *et al.* (2001).

5. FINAL REMARKS

A solution algorithm for the calculation of two-phase annular flow was successfully implemented. It solves the triangular relationship between the liquid film mass flow, wall shear stress and film thickness through an iterative procedure, taking advantage of the coupled solution of gas core and liquid film velocity profiles. In this way, no empirical closure correlation is used, and no velocity profile is assumed beforehand for the liquid film.

The model was successfully validated against the analytical solution for laminar flow and for a wide range of turbulent flow data of Wolf *et al.* (2001). For this, the turbulence model of Cioncolini *et al.* (2009) was used to compute the effective viscosities. Other turbulence models can be used, as long as they are based on turbulent viscosity.

As regards fully-developed flow, slight deviations between computed and experimental data can be observed for some flow conditions; however, these can be attributed to the turbulence modeling and/or entrainment correlations included in the model.

The results for developing annular flow are in good agreement with the experimental data, especially quantitatively, being all values within an absolute error of 15%. Improvement in this field is matter of current research, in order to achieve a better understanding and a more sophisticated modeling of the processes of entrainment and deposition, as well as to incorporate the effect of the gas phase expansion due to pressure changes along the duct. Implementation of a two-equation turbulence model suitable for developing annular flow is being carried out, using the algorithm hereby presented for the solution of the coupled equation system resulting from this model.

The solution algorithm presented in this work can be readily extended to deal with other annular flow calculations, such as heat transfer problems, evaporating film, etc., as long as the physical phenomena are properly modeled.

6. REFERENCES

Adechy, D. & Issa, R. I., 2004. Modelling of Annular Flow Through Pipes and T-Junctions, Computers & Fluids, Vol. 33, pp 289-313.

Alipchenkov, V. M.; Nigmatulin, R. I.; Soloviev, S. L.; Stonik, O. G.; Zaichik, L. I.; Zeigarnik, Y. A., 2004. A Three-Fluid Model of Two-Phase Dispersed-Annular Flow, International Journal of Heat and Mass Transfer, Vol. 47, pp 5323-5338.

Antal, S. P.; Kurul, N.; Podowski, M.; Lahey Jr, R. T., 1998. The Development of Multidimensional Modeling Capabilities for Annular Flows, Lyon, France.

Azzopardi, B. J., 1997. Drops in Annular Two-Phase Flow, International Journal of Multiphase Flow, Vol. 23, pp 1-53.

Cioncolini, A.; Thome, J. R.; Lombardi, C., 2009. Algebraic Turbulence Modeling in Adiabatic Gas-Liquid Annular Two-Phase Flow, International Journal of Multiphase Flow, Vol. 35, pp 580-596.

Dobran, F., 1983. Hydrodynamic and Heat Transfer Analysis of Two-Phase Annular Flow With a New Liquid Film Model of Turbulence, International Journal of Heat and Mass Transfer, Vol. 26, pp 1159-1171.

Fan, P.; Qiu, S. Z.; Jia, D. N., 2006. An Investigation of Flow Characteristics and Critical Heat Flux in Vertical Upward Round Tube, Nuclear Science and Techniques, Vol. 17, pp 170-176.

Fossa, M., 1995. A Simple Model to Evaluate Direct Contact Heat Transfer and Flow Characteristics in Annular Two-Phase Flow, International Journal of Heat and Fluid Flow, Vol. 16, pp 272-279.

Fu, F. & Klausner, J. F., 1997. A Separated Flow Model for Predicting Two-Phase Pressure Drop and Evaporative Heat Transfer for Vertical Annular Flow, International Journal of Heat and Fluid Flow, Vol. 18, pp 541-549.

Gill, L. E.; Hewitt, G. F.; Lacey, P. M., 1964. Sampling Probe Studies of the Gas Core in Annular Flow-II: Studies of the Effect of Phase Flow Rates on Phase and Velocity Distribution. Chemical Engineering Science, Vol. 19, pp 665-682.

Hewitt, G. F. & Whalley, P. B., 1989. Vertical Annular Two-Phase Flow, Multiphase Science and Technology, Vol. 4, pp 103-181.

Ishii, M. & Mishima, K., 1989. Droplet Entrainment Correlation in Annular Two-Phase Flow, International Journal of Heat and Mass Transfer, Vol. 32, pp 1835-1846.

Kataoka, I., Ishii, M., Nakayama, A.,2000. Entrainment and Deposition Rates of Droplets in Annular Two-Phase Flow, International Journal of Heat and Mass Transfer, Vol. 43, pp 1573-1589.

Kishore, B. N. & Jayanti, S., 2004. A Multidimensional Model for Annular Gas-Liquid Flow, Chemical Engineering Science, Vol. 59, pp 3577-3589.

Moeck, E. O. & Stachiewicz, J. W., 1972. A Droplet Interchange Model for Annular-Dispersed, Two-Phase Flow, International Journal of Heat and Mass Transfer, Vol. 15, pp 637-653.

Okawa, T. & Kataoka, I., 2005. Correlations for the Mass Transfer Rate of Droplets in Vertical Upward Annular Flow, International Journal of Heat and Mass Transfer, Vol. 48, pp 4766-4778.

Patankar, S. V., 1980. Numerical Heat Transfer and Fluid Flow, Hemisphere Publishing Corporation,

Patankar, S. V. & Spalding, D. B., 1972. A Calculation Procedure for Heat, Mass and Momentum Transfer in Three-Dimensional Parabolic Flows, International Journal of Heat and Mass Transfer, Vol. 15, pp 1787-1806.

Peng, S. W., 2008. Heat Flux Effect on the Droplet Entrainment and Deposition in Annular Flow Dryout, Communications in Nonlinear Science and Numerical Simulation, Vol. 13, pp 2223-2235.

Whalley, R. B. and Hewitt, G. F., 1978. The correlation of liquid entrainment fraction and entrainment rate in annular two-phase flow, Report No: 9187, Engineering Sciences Division, AERE Harwell.

Wolf, A.; Jayanti, S.; Hewitt, G. F., 2001. Flow Development in Vertical Annular Flow, Chemical Engineering Science, Vol. 56, pp 3221-3235.

7. RESPONSIBILITY NOTICE

The author(s) is (are) the only responsible for the printed material included in this paper.